PCCP

Accepted Manuscript

ROYAL SOCIETY OF CHEMISTRY

www.rsc.org/pccp

Journal Name

ARTICLE TYPE

Cite this: DOI: 10.1039/xxxxxxxxxx

Transition energies of benzoquinone anions are immune to symmetry breaking by a single water molecule†

Mark H Stockett*[a] and Steen Brøndsted Nielsen[a]

Received Date
Accepted Date

DOI: 10.1039/xxxxxxxxxx

www.rsc.org/journalname

_p_-Benzoquinone is the prototypical member of the quinone class of molecules with a basic functionality relevant for the primary reactions of photosynthesis. As electronically excited quinone anions are formed in near-resonant electron transfer, key issues are how the local environment affects excited-state energy levels and deexcitation times. The former we address here with action spectroscopy of mass-selected bare radical anions (_p_BQ$^-$) and one-water _p_BQ$^-$·H$_2$O complexes, isolated _in vacuo_. The complex represents a precursor for internal proton transfer to form the semiquinone free radical, the first chemical product in the light-driven electron transport chain. Both ions display bands in the visible and ultraviolet with, importantly, almost identical maxima. Despite localizing negative charge, thereby breaking the high orbital symmetries, water is surprisingly innocent. This finding implies that natural fluctuations in the quinone microenvironment cause only minor variations in excited-state energies and thus electron-transfer rates. Hence quinones are robust participants in electron transport.

The first chemical step in photosynthesis is the reduction of a quinone (plastoquinone) to a hydroquinone with a free-radical semiquinone as an intermediate[1]. This is catalyzed by light-driven electron transfer reactions in photosystem II: A light-harvesting complex funnels the excitation energy from antenna chlorophylls to a reaction-center chlorophyll where charge separation occurs as the chlorophyll transfers an electron to pheophytin (*i.e.*, a chlorophyll *a* that lacks magnesium). The latter donates the electron to protein-bound quinone. After two electron and proton transfers, hydroquinone is formed and released into the hydrophobic membrane region where it further participates in electron-transfer processes linking photosystem I and II together.

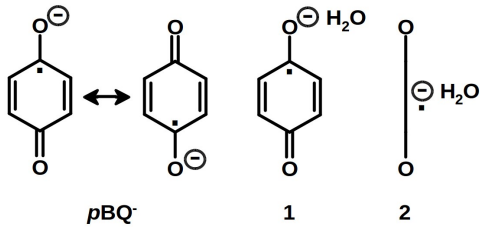

Fig. 1 Left: Resonance structures of _p_BQ$^-$ showing that the negative charge is delocalized. Right: **1** and **2** are possible structures of the _p_BQ$^-$·H$_2$O complex (structure **2** is shown viewed from the side). The water dipole localizes the charge in both cases.

para-Benzoquinone (*p*BQ, Figure 1) is the central moiety that accounts for the electron-accepting ability of quinones. It is therefore not surprising that the electronic properties of *p*BQ and the semiquinone radical anion (*p*BQ$^-$) have been studied in great detail[2–23]. While electron transfer to *p*BQ from a donor in theory is associated with a free-energy barrier in the Marcus inverted region, connecting the reactants to the products, there is strong evidence that rates can actually approach those of a barrier-less reaction[24]. To bypass the barrier requires a near-resonant electron transfer reaction, which implies that the quinone anion is produced in an electronically excited state upon electron acceptance. However, for the quinone to participate in electron transport it is then necessary that the anion quickly undergoes internal conversion to the electronic ground state to avoid autodetachment. Indeed, as beautifully demonstrated by Verlet and co-workers based on time-resolved photoelectron spectroscopy and ab initio calculations, excitation of bare *p*BQ$^-$ anions *in vacuo* at 400 nm and 480 nm yields excited states that decay on a sub-40 fs timescale via conical intersections[3]. Importantly, while some of the electronically excited anions undergo autodetachment, a significant

[a] *Department of Physics and Astronomy, Aarhus University, Aarhus, Denmark; E-mail: stockett@phys.au.dk*

† Electronic Supplementary Information (ESI) available: [details of any supplementary information available should be included here]. See DOI: 10.1039/b000000x/

fraction return through ultrafast internal conversion to the electronic ground state from where they undergo "slow" thermionic emission. Also of note is an older electron photodetachment experiment by Schiedt and Weinkauf on jet cooled pBQ$^-$ [16]. They reported a lifetime of the ^2A_u state to be less than 25 fs based on the width of a shape resonance at 2.50 eV (495 nm), in full accord with the result of Verlet and co-workers. This resonance lies well above the adiabatic detachment energy of 1.860 eV[16]. Finally, resonant electron attachment at electron energies of 0.7 eV and 1.35 eV produced pBQ$^-$ anions with lifetimes of several microseconds - the time scale for thermionic emission - clearly showing that internal conversion can compete with direct autodetachment [7,13,23]. Taken together, these results demonstrate that pBQ is excellent at both capturing and retaining electrons.

Now if excited states of quinone anions are indeed populated when receiving an electron from pheophytin, the rate could strongly depend on the immediate microenvironment of the quinone. A nearby water molecule could alter the state energies and thereby reduce the reaction rate as the states become non-resonant. Here, we have investigated this effect by performing electronic absorption spectroscopy experiments on both bare pBQ$^-$ ions and pBQ$^-$·H$_2$O complexes *in vacuo*. In the one-water complex, the water is either hydrogen bound to one of the two oxygens or it interacts with the π-electron cloud of the benzene ring, in both cases changing the electron distribution in the anion. Such local perturbations are often large for ions due to strong ion-dipole or ion-induced dipole interactions. For efficient electron transport, a certain robustness of the electron acceptor to the microenvironment and natural fluctuations is needed, and favourably, the excited-state energies should be unaffected by any local change taking place. This indeed seems to be the case as we show here that the electronic spectra of pBQ$^-$ and its one-water complex are nearly identical. We propose based on a number of spectroscopy studies on ion-molecule complexes that the limited effect of the microenvironment may very well be associated with the high symmetry of the quinone structure, providing another link between molecular structure and function.

The absorption by pBQ$^-$ anions *in vacuo* is obtained by measuring the photodepletion of the ions *versus* excitation wavelength. This is similar to previous gas-phase experiments by Brauman and co-workers and Weinkauf and co-workers [4,5,16], except that they detected the photoelectrons produced. The earlier experiment by Weinkauf was more sensitive to direct photodetatchment whereas ours probe both direct detachment and thermionic emission on longer timescales (up to 10 μs, see ESI†). No significant photofragmentation of pBQ$^-$ was observed; only electron loss occurred which depleted the ion beam signal. Our photodepletion spectrum is shown in Figure 2, along with an absorption spectrum obtained by Piech *et al.* in an Ar matrix [25]. The matrix spectrum has been blue-shifted by 0.07 eV, but otherwise the agreement in the width and position of the absorption bands is very good. The low resolution photodetachment spectrum of Brauman and co-workers is also similar to our depletion spectrum [4]. The beam depletion data are highly uncertain from 355 nm to 420 nm, due to limited laser power in this region. The low-energy band, generally assigned

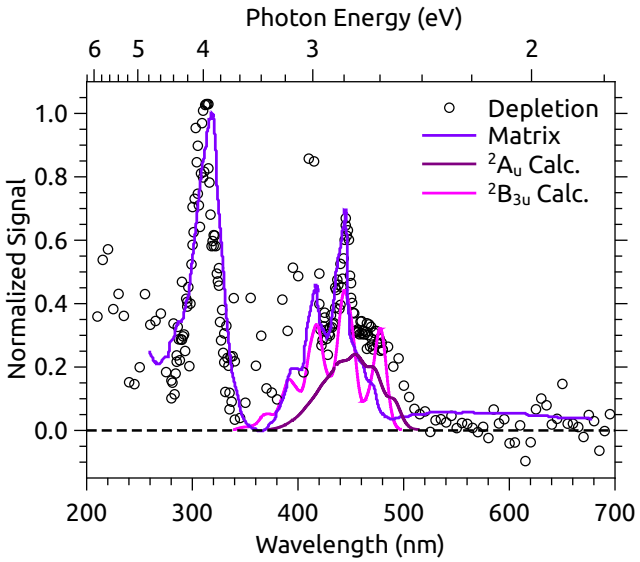

Fig. 2 The present photodepletion spectrum of pBQ$^-$ compared with the absorption spectrum obtained in an Ar matrix [25] and calculations of the ^2A_u and $^2B_{3u}$ band profiles [8]. The matrix spectrum has been blueshifted by 0.07 eV and the calculated spectra by 0.2 eV.

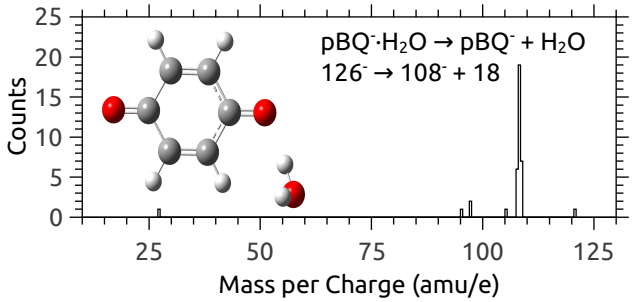

Fig. 3 Photo-induced dissociation (PID) mass spectrum for the pBQ$^-$·H$_2$O complex measured at 445 nm. Water loss is the only dissociation channel observed. The inset shows the DFT-optimized structure of pBQ$^-$·H$_2$O.

to a transition to the $^2B_{3u}$ state [3], has a maximum at 445 nm (2.79±0.05 eV). Relative to the matrix spectrum, our data show a more pronounced low-energy shoulder to the red of this band. Piech *et al.* [25] suggest this feature may be due to the broad ^2A_u shape resonance. This assignment is in good agreement with recent calculations and experiments [3,8,9]. It should also be noted that the ions in our experiments are hotter (room temperature) than those in the Ar matrix. There may thus be a contribution from unresolved hot bands to the shoulder in our gas-phase spectrum. For comparison, a calculation of the ^2A_u and $^2B_{3u}$ band profiles at 298 K (from Ref. [8] blue-shifted by 0.2 eV) are also shown in Figure 2. The agreement with our spectrum is very good, in support of the validity of the theoretical model.

The photo-induced dissociaton (PID) mass spectrum of the pBQ$^-$·H$_2$O complex measured at 445 nm is shown in Figure 3. Separation of the complex yielding pBQ$^-$ at m/z =108 (and H$_2$O) is the only dissociation channel observed. Laser power

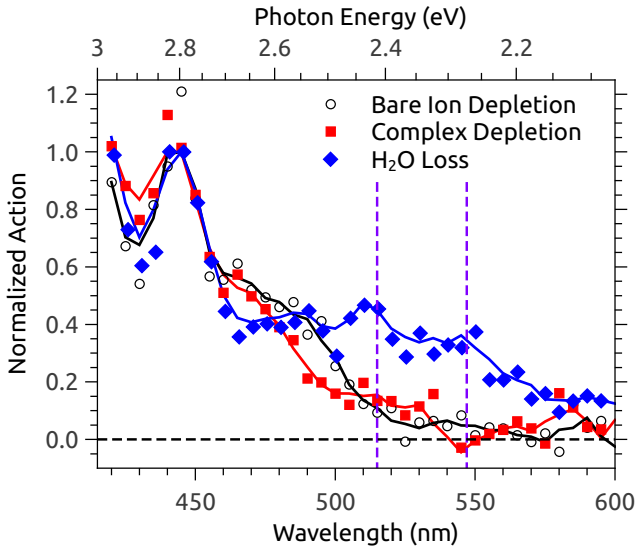

Fig. 4 Action spectra for pBQ$^-$ depletion, pBQ$^-$·H$_2$O depletion, and H$_2$O-loss from the pBQ$^-$·H$_2$O complex. Symbols are raw data and solid lines are 3-point moving averages. The dashed vertical lines show the positions of resonances from Ref[16].

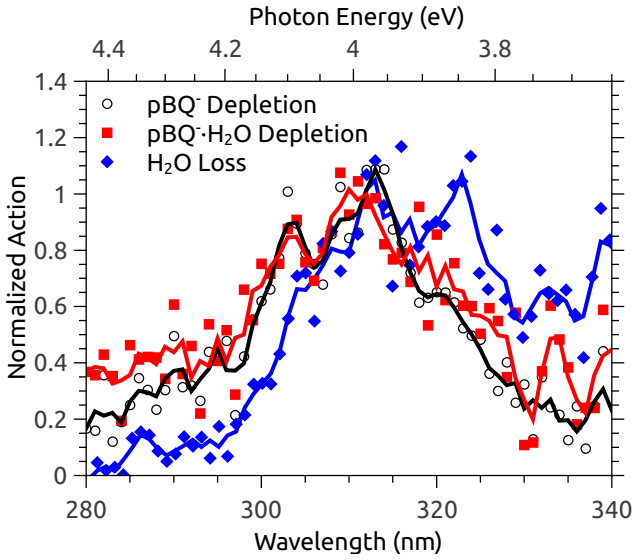

Fig. 5 Action spectra for pBQ$^-$ depletion, pBQ$^-$·H$_2$O depletion, and H$_2$O-loss from the pBQ$^-$·H$_2$O complex. Symbols are raw data and solid lines are 5-point moving averages.

dependence measurements (see ESI†) show that dissociation of the complex occurs after absorption of a single photon. Importantly, we see no OH$^-$ (m/z =17) corresponding to proton transfer from the water. Quantum chemical calculations performed at the B3LYP/6-311G(2d,p) level of density functional theory (DFT) also show that H$_2$O-loss is much more favorable than formation of OH$^-$, with dissociation energies of 0.62 eV and 4.61 eV, respectively.

Photo-depletion of the pBQ$^-$·H$_2$O ion beam was also measured. Relative to the total pBQ$^-$·H$_2$O beam depletion, H$_2$O-loss is a minor channel. Based on the relative action signals measured at 435 nm, we find that the observed water loss accounts for 0.5±0.1% of the total beam depletion, with the rest of the photo-excited ions undergoing direct electron detachment or thermionic emission.

Our DFT calculations give vertical and adiabatic electron detachment energies of 2.52 eV and 2.19 eV for the pBQ$^-$·H$_2$O complex and 2.06 eV and 1.85 eV for bare pBQ$^-$. The last value is in excellent agreement with the experimentally determined adiabatic electron affinity of 1.860±0.005 eV[16], lending support to the theoretical method, which was also used by Piech *et al.* for pBQ$^-$ [25]. The difference in adiabatic detachment energies (0.27 eV) is the binding energy of the H$_2$O to the neutral pBQ. All of these results pertain to structure **1** in Figure 1, where the water is bound to the oxygen atom of pBQ$^-$. No local minimum was found corresponding to structure **2**, hence this structure is likely not present in our experiments. The optimized geometry of the structure **1** is shown as an inset of Figure 3. Coordinates for optimized geometries and single point energies are given in the ESI†. The length of the hydrogen bond between the pBQ$^-$ and the H$_2$O is 1.74 Å, and increases to 2.01 Å in the neutral geometry, in good agreement with recent *ab initio* calculations which give 2.03 Å[26].

The addition of a single water molecule has surprisingly little effect on the lowest-energy electronic transitions of pBQ$^-$. This can be seen in Figure 4, where we compare our action spectra for pBQ$^-$ depletion, pBQ$^-$·H$_2$O depletion, and H$_2$O-loss from the pBQ$^-$·H$_2$O complex. The depletion spectra of pBQ$^-$ and pBQ$^-$·H$_2$O are nearly identical. In all cases a resonance is observed at 445 nm (2.8 eV). At longer wavelengths, some additional resonances are present in the the H$_2$O-loss spectrum. The positions of these resonances are in good agreement with those observed in photodetachment spectra of pBQ$^-$ by Schiedt and Weinkauf and identified as Feshbach resonances to the ^{2}B$_{2u}$ and ^{2}B$_{3g}$ states[16]. Relative to total pBQ$^-$·H$_2$O beam depletion, the yield of pBQ$^-$ increases to 2.0±1.5% at 515 and 545 nm, a factor of four higher than at the band maximum. The enhancement of these optically dark transitions may be due to the protective effect of evaporative cooling. Upon separation of the pBQ$^-$·H$_2$O complex, some of the excitation energy is taken away by the water molecule, making thermionic emission by the pBQ$^-$ less likely. Even small differences in survival probability of the pBQ$^-$ following water loss can evidently have significant effects on the yield of this minor channel. We have noted that the relative intensity of these low-energy resonances in the H$_2$O-loss spectrum vary somewhat with ion source conditions, probably due to small differences in the internal ion temperature.

As shown in Figure 5, the beam depletion spectra of the pBQ$^-$ and pBQ$^-$·H$_2$O in the region of the strong ultraviolet absorption band are nearly identical, each with band maximum near 312 nm (3.98±0.05 eV). This again shows that the electronic transition energy is unaffected by the addition of a single water molecule. The H$_2$O-loss spectrum, however, appears somewhat biased towards the red side of the band, with some additional action (but no clear band) further to the red. Once again, the relative yield of this minor channel (0.8±0.4% of the total beam depletion at 313 nm) depends sensitively on the internal energy of the pBQ$^-$·H$_2$O complex following ultrafast internal conversion. For this band, there may be an enhancement of the water-loss channel for exci-

tations to lower vibrational states than the Franck-Condon level, which lead in turn to less heating of the pBQ$^-$ following internal conversion. Even though water loss is a very minor channel, its observation unequivocally shows that internal conversion to the ground state has occurred even at this high excitation energy.

It is interesting to compare the results for pBQ$^-$ anions to other ions where the effect of a single solvent molecule on the electronic absorption band maximum has been determined. Permanganate anions (MnO_4^-) experience a shift in the lowest-energy transition of only 0.012 eV after attachment of a single water molecule while no observable shift is seen for tris(bipyridine)ruthenium(II) ($Ru(bipy)_3^{2+}$) dications by attachment of one acetonitrile molecule[27]. These two ions are, like pBQ$^-$, highly symmetric and possess no permanent dipole moment. Hence attachment of a solvent molecule necessarily lowers the symmetry, but with little effect on the excited state energies. In contrast, the *meta*-nitrophenolate[28] and oxyluciferin[29] anions display absorption blueshifted by 0.22 eV and 0.23 eV after attachment of a single water molecule; here the local environment plays a significant role as the negative charge is to a large extent localized at the phenolate oxygen prior to water binding. Excitation of the complex in these two cases moves electron density away from the charge site. The resulting loss of electrostatic interaction between the negative charge and the water dipole accounts for the blueshifted absorption. Such structural motifs are undesired in cases where robustness to the microenvironment is needed. They are, however, beneficial when colour modulation by a microenvironment is the goal. Taken together, it seems that high symmetry structural motifs are least affected. However, the amount of data is still limited, and more work to address this hypothesis is certainly needed.

Our work has shown that the electronic transition energies of isolated pBQ$^-$ anions are unaffected by a single water molecule over a remarkably broad energy region spanning more than 2 eV. This implies that pBQ$^-$ is a highly robust electron acceptor as the rate of electron transfer is governed by the matching of energy levels between the donor and acceptor species. This is particular important in the electron transport chain in photosynthesis where a quinone accepts an electron from pheophytin. Any fluctuations of the local environment of the quinone such as water attachment or dissociation are unlikely to have an effect on the electron transfer rate as the excited state energies are preserved. Not only does quinone have a high electron affinity, it is also a robust electron acceptor independent on the immediate environment, and it quickly undergoes internal conversion to the ground state after population of a state in the continuum.

We have performed beam depletion action spectroscopy on pBQ$^-$ and pBQ$^-\cdot H_2O$ ions isolated *in vacuuo*. The spectra of these two ions are nearly identical in both the visible and UV regions, strongly indicating that the electronic transition energies of pBQ$^-$ is unaffected by the addition of a single water molecule. This robustness against micro-environmental perturbations helps make pBQ an ideal electron acceptor. The minor pBQ$^-\cdot H_2O \rightarrow pBQ^-$ + H_2O channel is also observed at all transition energies, demonstrating that ultra-fast internal conversion is always competitive against direct photodetachment. The yield of this channel is highly sensitive to the internal energy of the complex following internal conversion.

Experimental and Theoretical Methods

All experiments were conducted with our experimental apparatus for action spectroscopy which has been described previously[30,31]. Briefly, pBQ$^-$ ions were produced by electrospray ionization (ESI) and stored in an octopole ion trap. Solvated pBQ$^-\cdot H_2O$ complexes were formed by continuously leaking water into the trap through a needle valve. The ions were gently extracted from the trap in 20-μs bunches at a rate of 40 Hz and accelerated to 50 keV. A bending magnet was used to select the ions of interest by their mass-to-charge ratio m/z. A frequency-tripled, Q-switched Nd:YAG laser combined with an optical parametric oscillator (OPO) produced $<$10-ns pulses in the range from 420 to 700 nm. These pulses were frequency doubled to produce light in the 210-355 nm range. A home-built sum-frequency generation module combines the 1064 nm YAG fundamental with the visible OPO pulses to produce light from 301 to 425 nm. Every second ion bunch was overlapped with a laser pulse in a collinear geometry and the action signal is the difference between the interleaved "laser on" and "laser off" signals. Ion bunch profiles for beam depletion and PID measurements are given in the ESI†. The laser power spectrum is measured periodically and used to correct our action spectra for laser power dependence (see ESI†). A hemispherical electrostatic energy analyzer placed after the interaction region was used to separate the product ions, which were counted with a channeltron detector.

Geometry optimization was performed at the B3LYP/6-311G(2d,p) level as implemented in Gaussian 09[32]. Vibrational frequencies were calculated to ensure that the structures correspond to local minima and not transition states. Electronic energies were corrected for zero-point kinetic energies (except for the calculation of vertical excitation energies).

Acknowledgements

The authors thank Simon Purup Eskildsen for performing DFT calculations. The authors acknowledge Villumfonden and the Danish Research Council for Independent Research (grant no. 4181-000488) for support.

References

1 J. M. Berg, J. L. Tymoczko and L. Stryer, in *Biochemistry*, Freeman, 2002, ch. 19.
2 C. W. West, J. N. Bull, E. Antonkov and J. R. Verlet, *J. Phys. Chem. A*, 2014, **118**, 11346–11354.
3 D. Horke, Q. Li, L. Blancafort and J. Verlet, *Nat. Chem.*, 2013, **5**, 711–717.
4 P. B. Comita and J. I. Brauman, *J. Am. Chem. Soc.*, 1987, **109**, 7591–7597.
5 J. Marks, P. B. Comita and J. I. Brauman, *J. Am. Chem. Soc.*, 1985, **107**, 3718–3719.
6 A. R. Cook, L. A. Curtiss, and J. R. Miller, *J. Am. Chem. Soc.*, 1997, **119**, 5729–5734.
7 M. Allan, *Chem. Phys.*, 1983, **81**, 235 – 241.
8 A. A. Kunitsa and K. B. Bravaya, *J. Phys. Chem. Lett.*, 2015, **6**, 1053–1058.
9 R. Pou-Amérigo, L. Serrano-Andrés, M. Merchán, E. Ortí and N. Forsberg, *Journal of the American Chemical Society*, 2000, **122**, 6067–6077.
10 Q. Fu, J. Yang and X.-B. Wang, *J. Phys. Chem. A*, 2011, **115**, 3201–3207.
11 M. O. El Ghazaly, A. Svendsen, H. Bluhme, S. Brøndsted Nielsen and L. H. Andersen, *Chem. Phys. Lett.*, 2005, **405**, 278–281.
12 S. Pshenichnyuk, G. Lomakin, A. Fokin, I. Pshenichnyuk and N. Asfandiarov, *Rapid Commun. Mass Spectrom.*, 2006, **20**, 383–386.
13 N. Asfandiarov, S. Pshenichnyuk, A. Fokin and E. Nafikova, *Chem. Phys.*, 2004, **298**, 263 – 266.

14 Y.-O. Kim, Y. M. Jung, S. B. Kim and S.-M. Park, *Anal. Chem.*, 2004, **76**, 5236–5240.
15 J. Weber, K. Malsch and G. Hohlneicher, *Chem. Phys.*, 2001, **264**, 275–318.
16 J. Schiedt and R. Weinkauf, *J. Chem. Phys.*, 1999, **110**, 304–314.
17 R. Gordon, D. Sieglaff, G. Rutherford and K. Stricklett, *Int. J. Mass Spectrom.*, 1997, **164**, 177–191.
18 K. Strode and E. Grimsrud, *Chem. Phys. Lett.*, 1994, **229**, 551–558.
19 A. Modelli and P. D. Burrow, *J. Phys. Chem.*, 1984, **88**, 3550–3554.
20 M. Allan, *Chem. Phys.*, 1984, **84**, 311–319.
21 C. Cooper, W. Naff and R. Compton, *J. Chem. Phys.*, 1975, **63**, 2752–2757.
22 P. Collins, L. Christophorou, E. Chaney and J. Carter, *Chemical Physics Letters*, 1970, **4**, 646–650.
23 L. Christophorou, J. Carter and A. Christodoulides, *Chem. Phys. Lett.*, 1969, **3**, 237–240.
24 G. L. Closs and J. R. Miller, *Science*, 1988, **240**, 440–447.
25 K. Piech, T. Bally, T. Ichino and J. Stanton, *Phys. Chem. Chem. Phys.*, 2014, **16**, 2011–2019.
26 T. Karsili, D. Tuna, J. Ehrmaier and W. Domcke, *Phys. Chem. Chem. Phys.*, 2015, DOI:10.1039/C5CP03831F.
27 M. H. Stockett and S. Brøndsted Nielsen, *J. Chem. Phys.*, 2015, **142**, 171102.
28 S. Brøndsted Nielsen, M. Brøndsted Nielsen and A. Rubio, *Acc. Chem. Res.*, 2014, **47**, 1417–1425.
29 K. Støchkel, C. N. Hansen, J. rgen Houmøller, L. Munksgaard Nielsen, K. Anggara, M. Linares, P. Norman, F. Nogueira, O. V. Maltsev, L. Hintermann, S. Brøndsted Nielsen, P. Naumov and B. F. Milne, *J. Am. Chem. Soc.*, 2013, **135**, 6485–6493.
30 K. Støchkel, B. F. Milne and S. Brøndsted Nielsen, *J. Phys. Chem. A*, 2011, **115**, 2155–2159.
31 J. A. Wyer and S. Brøndsted Nielsen, *Angew. Chem.*, 2012, **124**, 10402–10406.
32 M. J. Frisch, G. W. Trucks, H. B. Schlegel, G. E. Scuseria, M. A. Robb, J. R. Cheeseman, G. Scalmani, V. Barone, B. Mennucci, G. A. Petersson, H. Nakatsuji, M. Caricato, X. Li, H. P. Hratchian, A. F. Izmaylov, J. Bloino, G. Zheng, J. L. Sonnenberg, M. Hada, M. Ehara, K. Toyota, R. Fukuda, J. Hasegawa, M. Ishida, T. Nakajima, Y. Honda, O. Kitao, H. Nakai, T. Vreven, J. A. Montgomery, Jr., J. E. Peralta, F. Ogliaro, M. Bearpark, J. J. Heyd, E. Brothers, K. N. Kudin, V. N. Staroverov, R. Kobayashi, J. Normand, K. Raghavachari, A. Rendell, J. C. Burant, S. S. Iyengar, J. Tomasi, M. Cossi, N. Rega, J. M. Millam, M. Klene, J. E. Knox, J. B. Cross, V. Bakken, C. Adamo, J. Jaramillo, R. Gomperts, R. E. Stratmann, O. Yazyev, A. J. Austin, R. Cammi, C. Pomelli, J. W. Ochterski, R. L. Martin, K. Morokuma, V. G. Zakrzewski, G. A. Voth, P. Salvador, J. J. Dannenberg, S. Dapprich, A. D. Daniels, . Farkas, J. B. Foresman, J. V. Ortiz, J. Cioslowski and D. J. Fox, *Gaussian 09 Revision D.01*, Gaussian Inc. Wallingford CT 2009.